

**Structural studies (gas electron diffraction, vibrational spectra, He(I) photoelectron spectra (PES), and molecular orbital calculations) on gaseous methylenebis(phosphane),  $\text{CH}_2(\text{PH}_2)_2$ , and the PES of the series  $\text{CH}_2(\text{PXY})_2$  ( $\text{XY} = \text{HMe}, \text{HPr}^i, \text{HBu}^t, \text{Me}_2, \text{Pr}^i\text{Cl}, \text{Bu}^t\text{Cl}, \text{or Cl}_2$ ) \***

**Peter C. Knüppel, Gottfried Pawelke, Herbert Sommer, Othmar Stelzer \***,  
*Fachbereich 9, Anorganische Chemie, Bergische Universität-GH Wuppertal, 5600 Wuppertal 1 (B.R.D.)*

**Heinz Oberhammer \***,  
*Institut für Physikalische Chemie und Theoretische Chemie der Universität, 7400 Tübingen 1 (B.R.D.)*

**Michael F. Lappert \***, **Roger J. Suffolk**, and **John D. Watts**  
*School of Chemistry and Molecular Sciences, University of Sussex, Brighton BN1 9QJ (Great Britain)*  
(Received April 29th, 1988)

**Abstract**

Gaseous methylenebis(phosphane),  $\text{CH}_2(\text{PH}_2)_2$ , has been examined by a variety of techniques in order to establish its structure, including conformational preferences, and valence shell ionisation energies. The methods used have been those of gas electron diffraction (GED); infrared (IR), Raman (on the liquid), and He(I) photoelectron (PE) spectroscopy; and ab initio molecular orbital calculations. Although the MO calculations show that the  $C_{2v}$  ( $\tau 180^\circ$ ),  $C_2$ , and  $C_s$  conformers differ very little in energy (with  $C_{2v}$  marginally the most stable; giving an equilibrium distribution at  $25^\circ\text{C}$  of 31.7%  $C_{2v}$ , 37.6%  $C_2$ , and 30.7%  $C_s$  (SCF calculations with a DZP basis set and two sets of polarisation functions on phosphorus)), each item of the experimental data points to only a small ( $\leq 20\%$ ) contribution from the  $C_{2v}$  conformer. The GED results yield the following geometric parameters: C–H 1.064(12), P–H 1.428(5), P–C 1.854(2) Å; PCP 114.0(3), CPH 102.3(14), PCH 108.7(9), and the twist angle of  $\text{PH}_2$  groups around the P–C bond  $64(6)^\circ$ ; in good agreement with data obtained by calculations. The IR and Raman spectra were complemented by those obtained for  $\text{CH}_2(\text{PD}_2)_2$ . Complete assignments were made; a normal coordinate analysis was carried out, partly in order to provide

\* Dedicated to Professor Ernst Otto Fischer on the occasion of his 70th birthday.

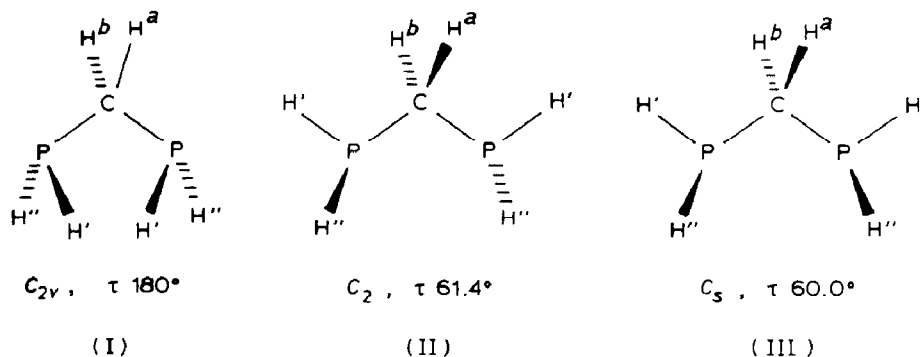
supporting evidence, but also to yield a comprehensive set of force constants. The PE spectrum was assigned, using (i) comparative data on  $\text{PH}_3$  and  $\text{PH}_2\text{Me}$ , (ii) relative intensities of bands, and (iii) data from *ab initio* calculations; the first bands at 9.55 and 9.80 are attributed to the antisymmetric and symmetric combinations of the two phosphorus lone pair orbitals ( $a$  and  $b$  in  $C_2$ , or  $a'$  and  $a''$  in  $C_s$ ), respectively. The PE spectra of other members of the series of methylenebis(phosphane)s  $\text{CH}_2(\text{PX}_2)_2$  ( $X = \text{Me}$  or  $\text{Cl}$ ) and  $\text{CH}_2(\text{PXY})_2$  ( $\text{XY} = \text{HMe}$ ,  $\text{HPr}^i$ ,  $\text{HBu}^t$ ,  $\text{Pr}^i\text{Cl}$ , or  $\text{Bu}^t\text{Cl}$ ) were obtained; these revealed unexceptional trends, attributable to  $+I$  effects  $\text{Bu}^t > \text{Pr}^i > \text{Me} > \text{H} > \text{Cl}(-I)$ , and additionally provided evidence that for the more bulky substituents the relative proportion of the  $C_{2v}$  conformer ( $\tau$   $180^\circ$ ) became more significant.

## Introduction

Methylenebis(phosphane)s,  $\text{CH}_2(\text{PXY})_2$ , are of considerable interest as mono- or bi-dentate ligands in transition metal chemistry [1,2]. Owing to their small bite angle, they may bridge metal atoms, and hence promote metal-metal interaction [3]. Methylenebis(phosphane)s bearing functional groups (H, Cl) at the phosphorus atoms are furthermore capable of inducing the formation of cluster compounds containing methylenephosphido(phosphane) ( $\text{R}_2\text{P}-\text{CH}_2-\overline{\text{P}}\text{R}$ ) or methylenebis(phosphido) ( $\text{RP}-\text{CH}_2-\overline{\text{P}}\text{R}$ ) bridging ligands [4].

In contrast to the well investigated coordination chemistry of  $\text{Ph}_2\text{P}-\text{CH}_2-\text{PPh}_2$  (dppm), and to a much lesser extent of other methylenebis(phosphane)s,  $\text{CH}_2(\text{PXY})_2$ , comparatively little is known about the structure of the free ligands  $\text{CH}_2(\text{PXY})_2$  [5]. Novikov, Koloméets, Golubinskii, Vilkov, Raevskii, Novikova, and Kurkin recently reported the gas electron diffraction (GED) structure of methylenebis(dichlorophosphane) [6a]. The GED structure of the oxide  $\text{CH}_2[\text{P}(=\text{O})\text{Cl}_2]_2$  has been studied by the same group [6b], whilst that of  $\text{CH}_2(\text{PMe}_2)_2$  was determined by Rankin, Robertson, and Karsch [7]. A vibrational analysis, by Novikov, Yarkov, Umarova, Raevskii, Kurkin, and Novikova of  $\text{CH}_2(\text{PCl}_2)_2$  revealed the presence of three conformers at ca.  $20^\circ\text{C}$  [6c].

It was therefore timely to obtain structural information on the parent methylenebis(phosphane),  $\text{CH}_2(\text{PH}_2)_2$ .



We now present results of such studies on gaseous  $\text{CH}_2(\text{PH}_2)_2$ , which comprise (i) the GED structure; (ii) a vibrational analysis (gaseous IR and liquid Raman), including data on  $\text{CH}_2(\text{PD}_2)_2$ ; (iii) the He(I) photoelectron spectrum [and that of some simple analogues  $\text{CH}_2(\text{PXY})_2$ ]; and (iv) ab initio molecular orbital calculations. Three conformations were considered, corresponding to molecules of  $C_{2v}$  (with a torsion angle of  $180^\circ$ ) (I),  $C_2$  (II), and  $C_s$  (III) symmetry.

## Experimental

### Synthesis

The methylenebis(phosphane)s  $\text{CH}_2(\text{PH}_2)_2$  [8],  $\text{CH}_2(\text{PXY})_2$  ( $X = \text{H}$  or  $\text{Cl}$ ;  $Y = \text{Me}$ ,  $\text{Pr}^i$ , or  $\text{Bu}^t$ ) [8],  $\text{CH}_2(\text{PMe}_2)_2$  [8,9], and  $\text{CH}_2(\text{PCl}_2)_2$  [4,8,10] were prepared by published procedures, and were purified by repeated distillations. Reduction of  $\text{CH}_2(\text{PCl}_2)_2$  with  $\text{Li}[\text{AlD}_4]$  afforded  $\text{CH}_2(\text{PD}_2)_2$ .

### Electron diffraction

The scattering intensities for  $\text{CH}_2(\text{PH}_2)_2$  were recorded with the Balzers Gasdiffractograph [11] at two camera distances (25 and 50 cm) with an accelerating voltage of ca. 60 kV. The electron wavelength was calibrated with ZnO powder diffraction patterns. The sample was kept at  $0^\circ\text{C}$  and the stainless steel inlet system and nozzle were at ambient temperature. The camera pressure never exceeded  $1.5 \times 10^{-5}$  mbar during the experiment. Exposure times were 4 to 6 and 20 to 40 s for the long and short camera distances, respectively. Two plates for each camera distance were analysed by the usual procedure [12]. The averaged modified molecular intensities in the ranges  $1.4 < s < 17$  and  $8 < s < 30 \text{ \AA}$  in steps of  $\Delta s = 0.2 \text{ \AA}^{-1}$  are presented in Fig. 1.

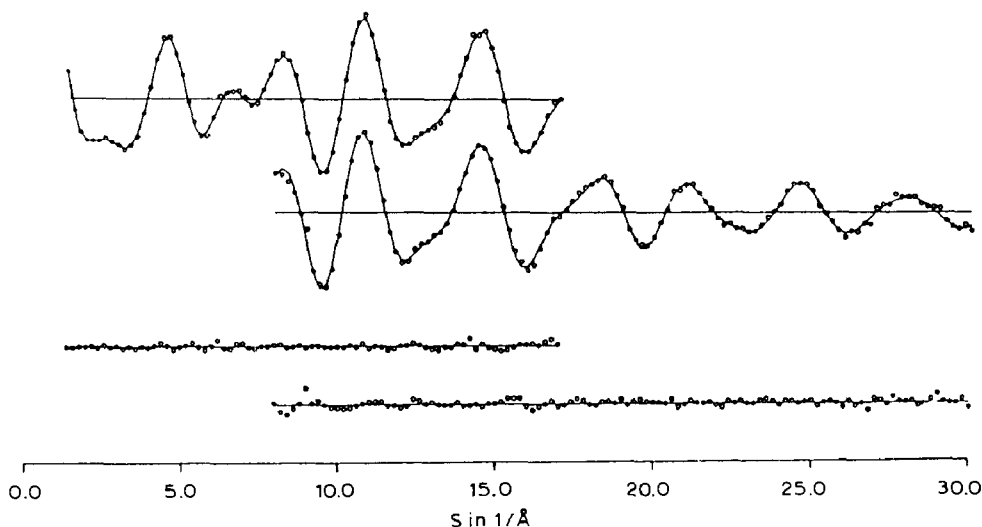


Fig. 1. Averaged modified molecular scattering intensity curve for methylenebis(phosphane),  $\text{CH}_2(\text{PH}_2)_2$ .

Table 1

He(I) photoelectron spectra of the methylenebisphosphanes  $\text{CH}_2(\text{PX}_2)_2$  ( $\text{X} = \text{H}, \text{Me}, \text{or Cl}$ ) and  $\text{CH}_2(\text{PXY})_2$  ( $\text{X} = \text{H or Cl}; \text{Y} = \text{Me}, \text{Pr}^i, \text{or Bu}^t$ )

$\text{CH}_2(\text{PXY})_2$	Ionisation energy (eV) <sup>a</sup>	Temperature (°C) <sup>b</sup>	Intensity (cps)
$\text{X} = \text{Y} = \text{H}$	9.55, 9.80, 12.50, 14.80	-75	$10^3$
$\text{X} = \text{Me}, \text{Y} = \text{H}$	8.95, 11.90, 14.20	-120	$4 \times 10^3$
$\text{X} = \text{Pr}^i, \text{Y} = \text{H}$	8.75, 12.10, 13.60	-52	$10^3$
$\text{X} = \text{Bu}^t, \text{Y} = \text{H}$	8.20, 9.40, 11.20, 12.00, 13.80	-41	$10^3$
$\text{X} = \text{Pr}^i, \text{Y} = \text{Cl}$	9.55, 11.40, 11.75, 12.70, 14.10	-46	$10^3$
$\text{X} = \text{Bu}^t, \text{Y} = \text{Cl}$	8.95, 10.30, 11.70, 12.95	+45	$10^3$
$\text{X} = \text{Y} = \text{Cl}$	9.75, 10.15, 11.85, 13.00, 13.85	-30	$4 \times 10^3$
$\text{X} = \text{Y} = \text{Me}$	8.45, 11.40, 13.80	-68	$4 \times 10^3$

<sup>a</sup> These are reproducible to  $\pm 0.05$  eV. <sup>b</sup> This refers to the temperature of the cooling bath containing the liquid sample of  $\text{CH}_2(\text{PX}_2)_2$  or  $\text{CH}_2(\text{PXY})_2$  from which the vapour was introduced into the PE spectrometer.

### Photoelectron spectra

The samples were treated as air- and moisture-sensitive. They were introduced into breakseal ampoules by use of a vacuum line. Each ampoule containing the appropriate sample was connected to the volatile inlet of the Perkin-Elmer PS16/18 photoelectron spectrometer, and was then evacuated. When the ampoule was opened, the vapour pressure of the sample was controlled by use of a slush bath, the relevant temperature of which is shown in the third column of Table 1. The He(I) photoelectron (PE) spectra were calibrated using argon and the He self-ionisation line.

### Vibrational spectra

Infrared (IR) spectra of the gaseous samples were recorded with a Nicolet 7199 FT spectrometer. The  $4000\text{--}400$   $\text{cm}^{-1}$  region was investigated with a resolution of  $0.5$   $\text{cm}^{-1}$ . Sample pressures in the 18.5 cm cells (equipped with KBr windows) varied between 1 and 60 mbar. Raman spectra of the liquid samples in 4 mm tubes were recorded on a Cary 82 spectrometer, using  $\text{Kr}^+$  excitation (6471 Å), 300 mW at the sample, and a slit-width of  $4$   $\text{cm}^{-1}$ .

## Results and discussion

### The gas electron diffraction analysis of $\text{CH}_2(\text{PH}_2)_2$

The radial distribution function for  $\text{CH}_2(\text{PH}_2)_2$  is shown in Fig. 2. The peaks for the three bonded distances (C-H, P-H, P-C) and for the non-bonded P...P distance are well separated. Calculations on models demonstrated that the experimental radial distribution function is incompatible with a  $C_{2v}$  structure, i.e. with twist angles around the P-C bonds of  $\tau 0^\circ$  or  $180^\circ$  (for  $\tau 0^\circ$ , the phosphorus lone pairs eclipse the opposite P-C bonds). For a  $C_{2v}$  model with  $\tau 180^\circ$ , the longest P...H distances (between phosphorus and the opposite phosphane hydrogens) occurred around 3.3 Å. The small peak at 4.2 Å was reproduced only with  $C_2$  or  $C_s$  models with a twist angle of ca.  $60^\circ$ . The  $C_2$  (twist angles in opposite directions) and  $C_s$  (twist angles in the same direction) structures differ merely by their long

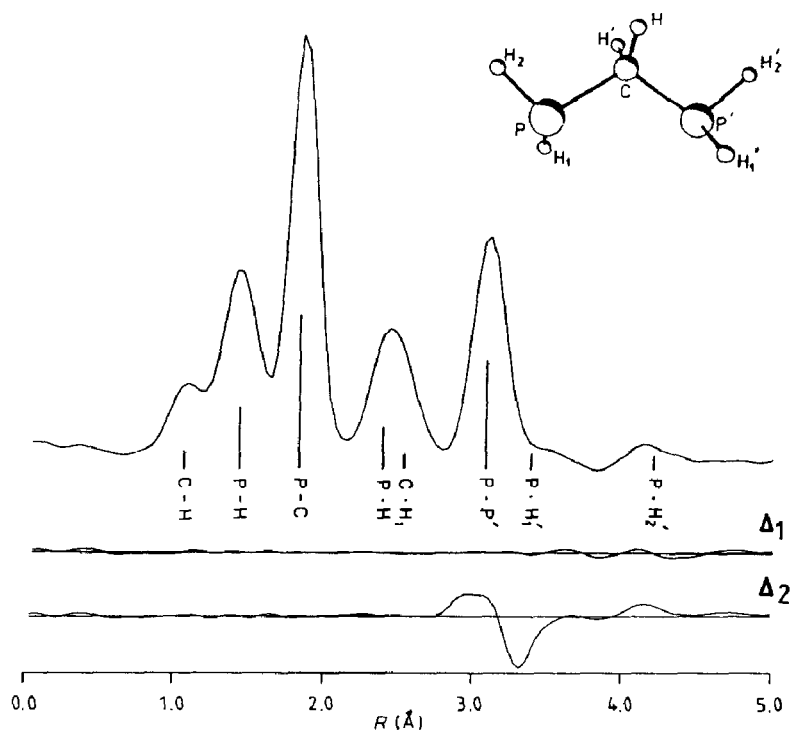


Fig. 2. Observed radial distribution (r.d.) curve for methylenebis(phosphane),  $\text{CH}_2(\text{PH}_2)_2$ , and the residual curve  $\Delta(\text{r.d.})$  (= expl. r.d. - calc. r.d.) for  $\text{C}_2$  ( $\Delta_1$ ), or ( $\Delta_2$ ) a mixture of 42%  $\text{C}_{2v}$  + 58%  $\text{C}_2$  conformers, respectively.

Table 2

Electron diffraction results for  $\text{CH}_2(\text{PH}_2)_2$  <sup>a</sup>

(a) Geometric parameters

C-H	1.064(12)	H-P-H	93.3 <sup>b</sup>
P-H	1.428(5)	P-C-H	108.7(9)
P-C	1.854(2)	H-C-H <sup>c</sup>	107.9(39)
P-C-P	114.0(3)	$\tau$ <sup>d</sup>	64 (6)
C-P-H	102.3(14)		

(b) Vibrational amplitudes <sup>e</sup>

C-H	0.063(14)	P...H'(1) } P...H'(2) }	0.16(4)
P-H	0.081(6)	H...H' } H(1)...H(2) }	0.11 <sup>b</sup>
P-C	0.052(3)	(H...H) <sub>long</sub>	0.20 <sup>b</sup>
P...P	0.083(4)		
P...H } C...H(1) }	0.075(15)		

(c) Agreement factors

$$R_{50} = 0.057 \quad R_{25} = 0.091$$

<sup>a</sup> Distances ( $r_g$ ) in Å and angles ( $r_a$ ) in degrees; error limits are  $3\sigma$  values. <sup>b</sup> Not refined. <sup>c</sup> Dependent parameter. <sup>d</sup> Twist angle of  $\text{PH}_2$  groups around P-C bond. The angle  $\tau$   $0^\circ$  corresponds to the  $\text{C}_{2v}$  configuration with the phosphorus lone pairs eclipsing the opposite P-C bonds. <sup>e</sup> Atom numbering is given in Fig. 2.

H...H distances between the two  $\text{PH}_2$  groups, which contribute little to the molecular intensities or radial distribution function. In the least squares analyses, the intensities were modified by a diagonal weight matrix [12], using the scattering amplitudes and phases of ref. 13. Assuming local  $C_s$  symmetry for the  $\text{PH}_2$  groups, the geometry of  $\text{CH}_2(\text{PH}_2)_2$  can be described by eight parameters ((a) in Table 2). The HPH angle was fixed at the value reported for  $\text{PH}_3$  [14]. Assumptions for vibrational amplitudes are evident from (b) in Table 2. In the final analysis, seven geometric parameters and six vibrational amplitudes were refined simultaneously. Three correlation coefficients had values larger than  $|0.5|$ :  $\text{PC}/\text{PCP} = -0.62$ ,  $\text{CH}/\text{PCH} = -0.70$ , and  $\text{CHP}/1 (\text{P}\dots\text{H}; \text{C}\dots\text{H}(1)) = -0.71$ . Refinements for  $C_2$  and  $C_s$  models resulted in identical geometric parameters and vibrational amplitudes. The  $R$  factors for the 50 cm data ( $R_{50}$ ) differed by less than 1%, and the  $R$  factors for the 25 cm data ( $R_{25}$ ) were equal. Thus, the electron diffraction data do not allow a distinction to be made between the  $C_2$  and  $C_s$  conformers, or a mixture of these conformers. The final results are summarised in Table 2.

In view of the results of the ab initio calculations (see below) which predict that the  $C_{2v}$  conformer ( $\tau$   $180^\circ$ ) is very slightly lower in energy than the  $C_2$  or  $C_s$  counterparts, it was decided to perform least squares analyses for various mixtures of  $C_{2v}$  and  $C_2$  models ( $C_s$  symmetry was not considered, since it is almost identical to  $C_2$  in the GED experiment). The geometric parameters were assumed to be the same for each conformer, except for the PCP angles for which the difference between  $C_{2v}$  and  $C_2$  structures was constrained to the ab initio value ( $10.3^\circ$ , see Table 6). Analyses with 10, 20, and 40% contributions of  $C_{2v}$  conformer led to increases of  $R_{50}$  ( $R_{25}$  was less sensitive toward these ratios) by 3.6, 21, and 140%, respectively. This demonstrates that a small contribution of a  $C_{2v}$  conformer cannot be excluded on the basis of the results of the GED experiment, but larger contributions ( $\geq 20\%$ ) are definitely ruled out. The difference curve for the mixture predicted by the first (SCF with DZP) ab initio calculations (42%  $C_{2v}$  and 58%  $C_2$  plus  $C_s$ ) is shown in Fig. 2.

Within experimental error the P-H and P-C bond lengths in  $\text{CH}_2(\text{PH}_2)_2$  are identical to those in  $\text{CH}_3\text{PH}_2$  (P-H = 1.423(7) and P-C = 1.858(3) Å) [15]. A comparison with GED results on  $\text{CH}_2(\text{PMe}_2)_2$  [7] and  $\text{CH}_2(\text{PCl}_2)_2$  [6a] demonstrates that  $C_2$  and  $C_s$  conformations are also preferred in these substituted methylenebis(phosphane)s. Whereas the presence of only a  $C_2$  conformer has been reported for the former ((P-C)<sub>mean</sub> 1.849(2) Å, PCP 113–18°, and  $\tau$  57(3)°) [7], a mixture of  $C_2$  (60 ± 12%) and  $C_s$  conformers was proposed for the latter (P-C 1.849(8) Å, PCP 111.2(13)°,  $\tau(C_2)$  69.9(19)° and  $\tau(C_s)$  49.8(50)°) [6a]. A similar mixture of  $C_2$  (63 ± 16%) and  $C_s$  conformers has also been reported for the analogous  $\text{P}^{\text{V}}$  compound  $\text{CH}_2[\text{P}(=\text{O})\text{Cl}_2]_2$ , with P-C 1.814(11) Å, CPC 114.4(23)°,  $\tau(C_2)$  53.5(20)°, and  $\tau(C_s)$  35.2(50)° [6b]. A considerably larger PCP angle of 122.6(10)° has been determined for  $\text{CH}_2[\text{P}(=\text{S})\text{F}_2]_2$  [16], which exists as a ca. 1/1 mixture of *gauche-gauche* ( $C_2$  symmetry) and *gauche-anti* ( $C_1$  symmetry) conformers.

#### *Vibrational spectra and normal coordinate analysis of $\text{CH}_2(\text{PH}_2)_2$*

A study of the vibrational spectra of  $\text{CH}_2(\text{PH}_2)_2$  and  $\text{CH}_2(\text{PD}_2)_2$  was undertaken in order to obtain an assignment of all the frequencies, and to gain further conformational information. As shown in Table 3, the polarisation state of the

Table 3

Vibrational spectra ( $\nu_{\max}$  in  $\text{cm}^{-1}$ ) of  $\text{CH}_2(\text{PH}_2)_2$  and  $\text{CH}_2(\text{PD}_2)_2$  <sup>a</sup>

$\text{CH}_2(\text{PH}_2)_2$		$\text{CH}_2(\text{PD}_2)_2$		Assignment	Calculated frequencies	Potential energy distribution
IR gas	Raman liquid	IR gas	Raman liquid			
2989 w	2949 m	2989 w	2949 m	$\nu_{12}$ (b)	2966/2966	(CH,101)
2932 w	2910 s p	2932 w	2910 s p	$\nu_1$ (a)	2928/2928	(CH,99)
2869 w	2865 w p	2869 w	2865 w p			
2800 vw	2800 w p					
	2770 w p		2770 w p			
2308 vs		1678 vs		$\nu_1/\nu_{15}$ (a)/(b)	2313/1659	(PH/PD,99)
2299 vs	2284 vs	1673 vs	1663 vs			
2282 vs	2275 vs p	1659 vs	1654 vs p	$\nu_3/\nu_{14}$ (a)/(b)	2291/1647	(PH/PD,101)
	1455 w p			$C_s$ -isomer		
1394 w	1388 m p		1388 m p	$\nu_5$ (a)	1393/1391	(HCH,77; PCH,16)
1158 w	1152 w	1144 m	1140 w	$\nu_{17}$ (b)	1154/1152	(PCH,109)
				$\nu_8$ (a)	1120	(HPH,83; PCH,15)
1130 w	1112 w			$\nu_{18}$ (b)	1118	(HPH,99)
1087 s	1074 m p				1096	(PCH,65; HPH,18; CPH,11)
		1074 m	1070 w p	$\nu_6$ (a)		
					1067	(PCH,100)
964 s				$\nu_{19}$ (b)	980	(CPH,93)
950 m	951 m p			$\nu_9$ (a)	957	(CPH,92)
903 s	892 m p			$\nu_{20}$ (b)	900	(CPH,86; CP,11)
798 m	794 m p			$\nu_{10}$ (a)	800	(CPH,106; PCH,36)
		836 s	835 w	$\nu_{18}$ (b)	820	(DPD,65; CP,15)
		796 s	782 m p	$\nu_8$ (a)	803	(DPD,95)
		788 s		$\nu_{13}$ (b)	778	(CP,60; PCH,20; CPD,19)
		751 s		$\nu_{19}$ (b)	763	(CPD,51; DPD,35; CP,17; PCH,15)
			749 s p	$\nu_9$ (a)	747	(CPD,70; CP,27)
739 s	735 m			$\nu_{13}$ (b)	737	(CP,103)
684 w	682 w	680 w		$\nu_{16}$ (b)	677	(PCH,88; CPH,24)
					666	(PCH, 36; CPD, 35; CP,16)
				$\nu_{10}$ (a)	604	(CPD,106; PCH,15)
		580 m	585 w p			
				$\nu_{20}$ (b)	588	(CPD,96; PCH,22)
	587 vs p	536 w	534 vs p	$\nu_2$ (a)	589/530	(CP,88; PCP,11)/
	244 w p		230 w p	$C_s$ -isomer		(CP,54; CPD,36)
	221 m p		214 m p	$\nu_7$ (a)	219/212	(PCP, 96; PCH, 17)/
						PCP,105; PCH,17)

<sup>a</sup> Abbreviations: s = strong, vs = very strong, w = weak, vw = very weak, m = medium, p = polarised.

Raman lines is not compatible with  $C_{2v}$  symmetry for the dominant conformer, but does not exclude a small contribution from such a  $C_{2v}$  conformer. Table 4 compares the distribution of normal modes for models having  $C_2$  and  $C_s$  symmetry. Significant differences in the polarisation states of lines should be especially apparent for the skeletal vibrations  $\nu_{\text{as}}(\text{CP}_2)$ ,  $\tau(\text{CH}_2)$ , and  $\omega(\text{CH}_2)$ , whereas the vibrations of the  $\text{PH}_2$  groups are expected to be less influenced by conformational changes. Since the Raman line which is clearly associated with  $\nu_{\text{as}}(\text{CP}_2)$  was definitely not polarised,  $C_2$  symmetry seems to be the best choice. However,  $\delta(\text{CP}_2)$  and  $\delta_s(\text{CH}_2)$  appeared as unsymmetrical doublets in the Raman spectra, and the less intense higher compo-

Table 4

Fundamental vibrations of  $\text{CH}_2(\text{PH}_2)_2$  for  $C_2$  and  $C_s$  symmetry

	$C_2$	$a$ (IR, Ra p)	$b$ (IR, Ra)	$C_s$	$a'$ (IR, Ra p)	$a''$ (IR, Ra)
$\nu(\text{CH})$		$\nu_1$	$\nu_{12}$		$\nu_1$	$\nu_{13}$
$\nu_s(\text{CP}_2)$		$\nu_2$			$\nu_2$	
$\nu_{as}(\text{CP}_2)$			$\nu_{13}$		$\nu_3$	
$\nu_s(\text{PH}_2)$		$\nu_3$	$\nu_{14}$		$\nu_4, \nu_5$	
$\nu_{as}(\text{PH}_2)$		$\nu_4$	$\nu_{15}$			$\nu_{14}, \nu_{15}$
$\delta_s(\text{CH}_2)$		$\nu_5$			$\nu_6$	
$\tau(\text{CH}_2)$		$\nu_6$				$\nu_{16}$
$\rho(\text{CH}_2)$			$\nu_{16}$			$\nu_{17}$
$\omega(\text{CH}_2)$			$\nu_{17}$		$\nu_7$	
$\delta(\text{CP}_2)$		$\nu_7$			$\nu_8$	
$\delta_s(\text{PH}_2)$		$\nu_8$	$\nu_{18}$		$\nu_9, \nu_{10}$	
$\omega(\text{PH}_2)$		$\nu_9$	$\nu_{19}$		$\nu_{11}, \nu_{12}$	
$\rho(\text{PH}_2)$		$\nu_{10}$	$\nu_{20}$			$\nu_{18}, \nu_{19}$
$\tau(\text{PH}_2)$		$\nu_{11}$	$\nu_{21}$			$\nu_{20}, \nu_{21}$

nents may be attributed to the  $C_s$  isomer. In the following account, the spectra of  $\text{CH}_2(\text{PH}_2)_2$  and  $\text{CH}_2(\text{PD}_2)_2$  are discussed on the assumption of  $C_2$  symmetry.

The  $\nu_1(\text{CH})$  and  $\nu_{12}(\text{CH})$  stretching vibrations are unambiguously assigned to the Raman lines at 2910 and 2949  $\text{cm}^{-1}$ , whereas the PH(PD) stretching fundamentals  $\nu_4/\nu_{15}$  and  $\nu_3/\nu_{14}$  are believed to be the bands at 2284(1663) and 2275(1634)  $\text{cm}^{-1}$ , respectively. The four  $\text{CH}_2$  bending vibrations are assigned by comparison with the analogous fundamentals of  $\text{CH}_2\text{Br}_2$ :  $a_1$  1379  $\text{cm}^{-1}$ ,  $a_2$  1090  $\text{cm}^{-1}$ ,  $b_2$  1191  $\text{cm}^{-1}$ , and  $b_1$  810  $\text{cm}^{-1}$  [17]. Two polarised bands, at 1388 and 1074  $\text{cm}^{-1}$ , were unshifted upon deuteration of the  $\text{PH}_2$  groups; they are assigned to the scissor and twisting modes,  $\nu_5$  and  $\nu_6$ . Another only slightly shifted band was located at 1152  $\text{cm}^{-1}$ , and is ascribed to  $\nu_{17}$ . The  $\nu_{16}$  mode is expected to fall below 800  $\text{cm}^{-1}$ , which is appropriate for  $\text{PH}_2$  bending. The  $\text{PH}_2$  scissor vibrations,  $\nu_8$  and  $\nu_{18}$ , are allocated to the Raman line at 1112  $\text{cm}^{-1}$ ; it was shifted to 838  $\text{cm}^{-1}$  in  $\text{CH}_2(\text{PD}_2)_2$ . Three other strong bands, at 951, 892, and 794  $\text{cm}^{-1}$ , were not observed in the deuterated species, and are therefore assigned to  $\nu_9$ ,  $\nu_{20}$ , and  $\nu_{10}$ . A strong IR absorption (which coincided with a depolarised Raman line) at 739  $\text{cm}^{-1}$  is identified as  $\nu_{13}$  ( $\nu_{as}(\text{CP}_2)$ ), whereas the symmetric counterpart,  $\nu_2$ , is assigned to the very strong Raman line at 587  $\text{cm}^{-1}$ . The  $\nu_{16}$  mode is identified as the weak line observed at 682  $\text{cm}^{-1}$ . In  $\text{CH}_2(\text{PD}_2)_2$ , the  $\text{PD}_2$  bending modes appear to be coupled with  $\nu_{16}$  and the stretching vibrations  $\nu_2$  and  $\nu_{13}$ . They may therefore best be described by their potential energy distribution, as shown in Table 3. The unsymmetrical doublet of lines at 244/221 and 230/214  $\text{cm}^{-1}$  in  $\text{CH}_2(\text{PH}_2)_2$  and  $\text{CH}_2(\text{PD}_2)_2$ , respectively, are assigned to the skeletal bending mode  $\nu_7$ ; the higher, less intense, component is tentatively attributed to the  $C_s$  isomer. There was no evidence for absorptions due to the torsions  $\nu_{11}$  and  $\nu_{21}$ , but in any event they are expected to lie below 200  $\text{cm}^{-1}$ .

The major aim of the normal coordinate analysis was to confirm and to support the above assignments. The calculations were performed with the programme NORCOR [18], using the GED structural parameters of Table 2. Force constants were transferred from  $\text{CH}_3\text{PH}_2$  [19] and fitted to the observed frequencies as far as



Table 5

Inner diagonal force constants ( $\times 10^2 \text{ N m}^{-1}$ ) scaled to 100 pm of  $\text{CH}_2(\text{PH}_2)_2$  and  $\text{CH}_3\text{PH}_2$  [19]

Assignment	$\text{CH}_2(\text{PH}_2)_2$	$\text{CH}_3\text{PH}_2$
$f(\text{CP})$	2.900	2.882
$f(\text{CH})$	4.760	4.765
$f(\text{PH})$	3.051	3.082
$f(\text{PCP})$	0.762	
$f(\text{PCH})$	0.511	0.503
$f(\text{HCH})$	0.461	
$f(\text{HPH})$	0.743	0.682
$f(\text{CPH})$	0.945	0.808

seemed reasonable. A comparison of the final diagonal force constants for  $\text{CH}_2(\text{PH}_2)_2$  with those of  $\text{CH}_3\text{PH}_2$  [19] is shown in Table 5. A complete set of force constants is available on request (from O.S.).

*He(I) Photoelectron spectra of  $\text{CH}_2(\text{PX}_2)_2$  ( $X = \text{H}, \text{Me}, \text{or Cl}$ ) and  $\text{CH}_2(\text{PXY})_2$  ( $\text{XY} = \text{HMe}, \text{HPr}^i, \text{HBu}^t, \text{Pr}^i\text{Cl}, \text{or Bu}^t\text{Cl}$ )*

Molecular orbital calculations have already been carried out on a series of molecules  $\text{CH}_2(\text{X}')\text{Y}'$  ( $\text{X}'$  and  $\text{Y}'$  were selected from  $\text{NH}_2$ ,  $\text{OH}$ ,  $\text{F}$ ,  $\text{PH}_2$ ,  $\text{SH}$ , and  $\text{Cl}$ ) to determine whether anomeric effects, well established for first row substituents  $\text{X}$  and  $\text{Y}$ , also exist for their second row congeners ( $\text{PH}_2$ ,  $\text{SH}$ , and  $\text{Cl}$ ) [20]; Jemmis, Schleyer, and Spitznagel concluded that the latter are greatly attenuated relative to the former. (Their method of investigation focussed on (i) methyl stabilisation energies:  $\text{CH}_4 + \text{CH}_2(\text{X}')\text{Y}' \rightarrow \text{CH}_3\text{X}' + \text{CH}_3\text{Y}'$ , and (ii) conformational preferences; but no explicit comments relating to (ii) were made for  $\text{CH}_2(\text{PH}_2)_2$ .)  $\text{He(I)}$  photoelectron spectra also offer a sensitive probe into  $\ddot{\text{X}}'/\ddot{\text{Y}}'$  lone-pair interactions in such molecules. The present data on the series  $\text{CH}_2(\text{PX}_2)_2$  ( $X = \text{H}, \text{Me}, \text{or Cl}$ ) and  $\text{CH}_2(\text{PXY})_2$  ( $\text{XY} = \text{HMe}, \text{HPr}^i, \text{HBu}^t, \text{Pr}^i\text{Cl}, \text{or Bu}^t\text{Cl}$ ) are illustrated in Fig. 3, and the principal features are presented in Table 1.

The reference compound for both series is methylenebis(phosphane),  $\text{CH}_2(\text{PH}_2)_2$ ; accordingly its  $\text{He(I)}$  PE spectrum is first considered. The GED study (vide supra) showed that the radial distribution function is not compatible with  $\text{C}_{2v}$  symmetry; rather that  $\text{CH}_2(\text{PH}_2)_2$  exists in the gas phase in  $\text{C}_2$  or  $\text{C}_s$ , or a mixture of  $\text{C}_2$  and  $\text{C}_s$ , conformers, with possibly a small ( $\leq 20\%$ ) contribution from the  $\text{C}_{2v}$  ( $\tau 180^\circ$ ) conformer. For the  $\text{C}_2$  species (II) the phosphorus lone pairs are in a *gauche* relationship and for the  $\text{C}_s$  species, (III), they are eclipsed. In a previous study of a wide range of monophosphanes  $\text{PXYZ}$  [21], the first PE band was attributed to the removal of an electron from the phosphorus lone pair orbital. In  $\text{PH}_3$ , the value was 10.58 eV [22], in  $\text{PMe}_3$  8.63 eV [21],  $\text{PBu}_3$  7.70 eV, and  $\text{PMe}_2\text{Cl}$  9.19 eV. In a bis(phosphane), the two phosphorus lone pairs are expected to interact in either a symmetric or asymmetric fashion to give rise to two bands, with the magnitude of their separation depending on the degree of interaction between the lone pairs. We note that for diphosphanes with adjacent phosphorus-centred lone pairs, such separation was found to be 1.68 eV for *trans*- $\text{P}_2\text{Me}_4$  [23] and 1.40 eV for *trans*- $\text{P}_2(\text{CF}_3)_4$  [24], but was much less in the *gauche* isomers.

In the PE spectrum of  $\text{CH}_2(\text{PH}_2)_2$  (Fig. 3a), a broad first band was centred at

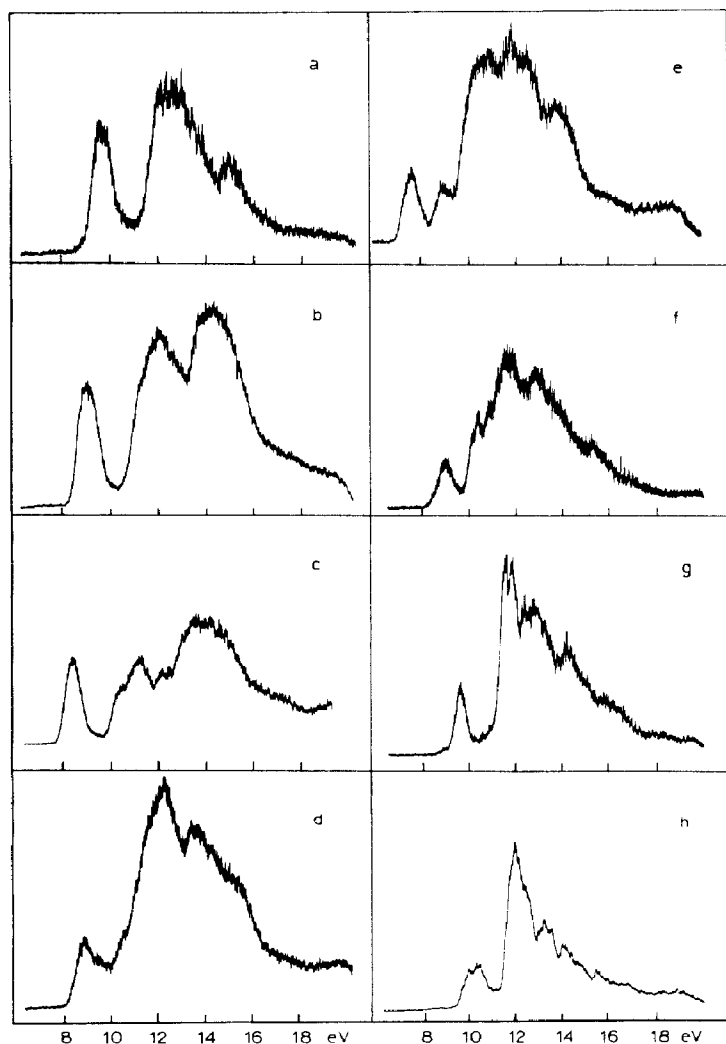


Fig. 3. He(I) photoelectron spectra for  $\text{CH}_2(\text{PH}_2)_2$  (a) and  $\text{CH}_2(\text{PXY})_2$  ( $\text{XY} = \text{HMe}$  (b),  $\text{HPr}^i$  (c),  $\text{HBu}^t$  (d),  $\text{Me}_2$  (e),  $\text{Pr}^i\text{Cl}$  (f),  $\text{Bu}^t\text{Cl}$  (g), or  $\text{Cl}_2$  (h)).

ca. 9.55 eV (with a shoulder at 9.80 eV), followed by a large energy gap before the onset of the second ionisation feature centred at 12.50 eV. The ab initio calculations (see below and Table 7) showed that for the molecule in a  $C_{2v}$  configuration the phosphorus lone pair orbitals are expected to be split by almost 2 eV, whereas in the  $C_2/C_s$  case, this splitting is only ca. 0.2 eV. The integrated intensity of the first two bands is approximately 1/2; on this basis, and keeping in mind the GED and vibrational spectral results, we conclude that both phosphorus lone pair orbitals are located in the first band. Were this not the case, then the intensity of the 9.55 eV band would be much lower, probably about half of the observed value. The identification of discrete bands arising from separate  $C_2$  or  $C_s$  conformers was not possible; in any event, calculations suggest that they would differ by only ca. 0.05 eV, which is close to the experimental limit of resolution.

The second band, centred at 12.50 eV, is assigned to ionisation from the P–H  $\sigma$  bonds; calculations predicted that these would be spread over almost 3 eV in the

$C_2/C_s$  case, consistent with the experimental spectrum. The third band, at ca. 14.80 eV, is estimated to have ca. half the intensity of that at 9.55 eV. It is assigned to ionisation from the first C–H  $\sigma$  orbital, predicted to be at 16.3/16.4 eV. The remaining three orbitals ( $a$ ,  $b$ ,  $a$  for  $C_2$ ; or  $a'$ ,  $a''$ ,  $a'$  for  $C_s$ ; Table 7) are believed to be submerged in the background up to 21 eV.

The next compound to be discussed is  $\text{CH}_2(\text{PHMe})_2$ . The PE spectrum (Fig. 3b) gave no evidence for clear-cut splitting of the first band; and the main noteworthy feature was the shift of this band to lower energy by ca. 0.60 eV compared with  $\text{CH}_2(\text{PH}_2)_2$ . This is a consequence of the positive inductive effect of the two methyl groups; the magnitude of the shift is consistent with the above data on  $\text{PMe}_3$  and  $\text{PH}_3$ . We draw attention to the marked increase in intensity of the band centred at 14.20 eV compared with that at 14.80 eV in  $\text{CH}_2(\text{PH}_2)_2$ ; this is attributed to the presence of the methyl (C–H)- $\sigma$ -orbitals.

Within the series  $\text{CH}_2(\text{PH}_2)_2$ ,  $\text{CH}_2(\text{PHMe})_2$ , and  $\text{CH}_2(\text{PMe}_2)_2$ , the shift in the first ionisation energy (IE) is evidently not linearly additive; thus  $\text{CH}_2(\text{PMe}_2)_2$  (Fig. 3c) showed a further shift of 0.50 eV. For  $\text{CH}_2(\text{PHPr}^i)_2$  (Fig. 3d), the first IE was 0.80 eV lower in energy than for  $\text{CH}_2(\text{PH}_2)_2$ ; once more there was little evidence for splitting of this first band.

For  $\text{CH}_2(\text{PHBu}^t)_2$  (Fig. 3e), the first IE was shifted by 1.35 eV to lower energy than for  $\text{CH}_2(\text{PH}_2)_2$ , but there was now a small feature present at 9.40 eV of similar intensity to the first band at 8.20 eV. Their separation of 1.20 eV is too large to be due to the splitting of the two phosphorus lone pair orbitals in a molecule of  $C_2$  or  $C_s$  symmetry for the  $\text{>P-C-P<}$  skeleton, indicating that the skeleton may have in larger part adopted a  $C_{2v}$  arrangement, in which the phosphorus lone pair are eclipsed owing to the bulky nature of the  $\text{Bu}^t$  groups. The relative intensities of the 9.40 and 8.20 eV bands is such that a 60–70% contribution from a  $C_{2v}$  conformer is plausible.

Comparing the PE spectrum of  $\text{CH}_2(\text{PClBu}^t)_2$  (Fig. 3f) with that of  $\text{CH}_2(\text{PHBu}^t)_2$ , it is evident that the first IE is 0.75 eV greater in the former, attributable to  $-I$  effect of the chlorine atoms. In addition to the band at 8.95 eV, there was a shoulder at 10.30 eV, and this may also be due to a similar splitting of the phosphorus lone pair orbitals in the  $C_{2v}$  conformer. The separation of 1.35 eV between the first two IEs compares with 1.20 eV for  $\text{CH}_2(\text{PHBu}^t)_2$ .

The PE spectrum of  $\text{CH}_2(\text{PClPr}^i)_2$  (Fig. 3g) did not show any evidence for lone pair splitting. The main feature was the shift of the first IE by 0.80 eV to higher energy compared with  $\text{CH}_2(\text{PHPr}^i)_2$  due to the  $-I$  effect of the chlorine atoms. Finally, for  $\text{CH}_2(\text{PCl}_2)_2$  (Fig. 3h), there was some evidence for a small splitting occurring at 9.75 and 10.15 eV; this may be due to distinct  $C_2$  or  $C_s$  conformers.

We recognise that the molecules  $\text{CH}_2(\text{PXY})_2$  where  $X \neq Y$  exist as both meso and rac diastereoisomers, but these are not distinguishable from their PE spectra.

#### *Ab initio calculations*

To complement our experimental work we have also carried out some ab initio MO calculations on methylenebis(phosphane). These calculations were undertaken with the aim of determining (i) the most stable conformers and appropriate geometrical parameters (Table 6), and (ii) the valence ionisation energies (Table 7). While the communication by Von R. Schleyer and coworkers [20] addresses point (i) in principle, it presents no conclusion for  $\text{CH}_2(\text{PH}_2)_2$ .

Table 6

Geometrical parameters from the ab initio MO calculations for the three conformers of methylenebis(phosphane),  $\text{CH}_2(\text{PH}_2)_2$ , compared with the GED data. Bond lengths in Å, angles in degrees.

Distance or angle	Electron diffraction data	Calculated parameters		
		$C_{2v}$	$C_2$	$C_s$
$r(\text{C-H})$	1.064(12)	1.087	1.084	1.084
$r(\text{P-H})$	1.428(5)	1.406	1.405	1.407
$r(\text{P-C})$	1.854(2)	1.860	1.864	1.864
PCP	114.0(3)	122.1	111.8	111.8
HPC	102.3(14)	99.2	98.6	98.4
HPH	93.3 <sup>a</sup>	95.4	95.4	95.2
HCP	108.7(9)	107.1	109.3	109.2
HCH	107.9(39)	105.0	107.7	107.9
$\tau$	64(6)	180.0	61.4	60.0

<sup>a</sup> Assumed.

Initial calculations were carried out at the SCF level with a double- $\zeta$  plus polarisation (DZP) Gaussian basis set. The carbon and hydrogen double- $\zeta$  basis sets comprised Dunning's  $4s2p$  and  $2s$  contractions of  $9s5p$  and  $4s$  primitive sets [25]. To these double- $\zeta$  basis sets were added (i) a set of  $d$  functions having an exponent of 0.75 (for C) and (ii) a set of  $p$  functions with an exponent of 1.0 (for H) [26]. Our phosphorus basis set comprised McLean and Chandler's  $6s4p$  contraction of a  $12s9p$  primitive set [27] augmented with a set of  $d$  functions having exponent 0.55 [28].

To determine the lowest energy conformations of the molecule, we studied various  $C_{2v}$ ,  $C_2$ , and  $C_s$  structures. The geometries of the different conformers were optimised by standard analytic gradient techniques [29,30]. Apart from the maintenance of the appropriate molecular symmetry, no other constraints were applied in the geometry optimisations. Once a stationary point was located, its nature (e.g., local minimum or transition state) was determined by computation of harmonic vibrational frequencies [31].

Table 7

Ionisation energies (eV) from the ab initio MO calculations for the three conformers of methylenebis(phosphane),  $\text{CH}_2(\text{PH}_2)_2$ , with assignments in parentheses

$C_{2v}$	$C_2$	$C_s$
9.012 ( $b_2$ )	9.825 ( $a$ )	9.800 ( $a'$ )
10.905 ( $a_1$ )	9.993 ( $b$ )	10.059 ( $a''$ )
13.596 ( $a_1$ )	12.615 ( $b$ )	12.688 ( $a''$ )
13.695 ( $b_1$ )	13.579 ( $a$ )	13.326 ( $a'$ )
14.120 ( $a_2$ )	14.132 ( $b$ )	14.350 ( $a''$ )
14.140 ( $b_2$ )	15.581 ( $a$ )	15.579 ( $a'$ )
16.722 ( $b_1$ )	16.342 ( $b$ )	16.472 ( $a'$ )
21.377 ( $a_1$ )	21.056 ( $a$ )	21.095 ( $a'$ )
22.845 ( $b_2$ )	22.925 ( $b$ )	22.916 ( $a''$ )
27.446 ( $a_1$ )	27.403 ( $a$ )	27.417 ( $a'$ )

Estimates of the molecular ionisation energies were obtained straightforwardly by Koopmans' theorem [32].

Our search of the rotational potential energy surface of methylenebis(phosphane) yielded three energy minima, all of similar energy. The lowest energy conformer was predicted to be of  $C_{2v}$  symmetry ( $\tau$  180°). The  $C_2$  and  $C_s$  conformers were predicted to be respectively 2.2 and 3.2 kJ mol<sup>-1</sup> higher in energy. These energy differences indicate that at equilibrium methylenebis(phosphane) exists as mixture of these three conformers. Since the  $C_2$  and  $C_s$  conformers both have two equivalent minima, at 25 °C (the nozzle temperature in the GED experiment) the equilibrium percentages of the conformers are 42%  $C_{2v}$ , 35%  $C_2$ , and 23%  $C_s$ . This is somewhat at odds with the experimental GED data (also those based on vibrational or PE spectra) which allow for only a small contribution from the  $C_{2v}$  conformer ( $\leq$  20%). In view of this discrepancy, some further calculations were undertaken.

Firstly, the effect of electron correlation was estimated by carrying out fourth-order Moller-Plesset perturbation theory (MP4) calculations [28]. These calculations used the DZP basis described above and were done at the DZP SCF optimum geometry. Like the SCF calculations, they predicted the  $C_{2v}$  conformer to be the most stable, giving relative energies of 4.1 and 4.2 kJ mol<sup>-1</sup> for the  $C_2$  and  $C_s$  conformers.

Next, we made a series of calculations with the well known 6-31G\*\* basis set [28]. This basis has been well calibrated [28] and would be expected to give similar results to our DZP basis set. As with the latter, we carried out geometry optimisations at the SCF level and followed these with MP4 calculations at the optimum geometries. Once again, in both sets of calculations the  $C_{2v}$  conformer was predicted to be the most stable. The SCF calculations predicted the  $C_2$  and  $C_s$  conformers to be 1.9 and 2.5 kJ mol<sup>-1</sup> higher in energy, while the MP4 energy differences were 3.0 and 2.8 kJ mol<sup>-1</sup>, respectively.

We then carried out SCF calculations with the 6-31 + + G\*\* basis set [28], at the 6-31G\*\* optimum geometries. This basis set contains diffuse *s* and *p* functions which may give a better description of the phosphorus lone pair orbitals. These calculations also predicted the  $C_{2v}$  conformer to be the most stable; the  $C_2$  and  $C_s$  conformers were predicted to be 2.0 and 2.9 kJ mol<sup>-1</sup>, respectively, higher in energy.

In a final effort to reconcile theory with experiment, we carried out SCF calculations with a DZP basis set with two sets of polarisation functions on phosphorus, exponents 1.0 and 0.25. These calculations used the DZP optimum geometry and again predicted the  $C_{2v}$  conformer to be the most stable, but the energy differences between the  $C_{2v}$  and  $C_2$  conformers and between the  $C_{2v}$  and  $C_s$  conformers were predicted to be only 1.3 and 1.8 kJ mol<sup>-1</sup>, respectively. These energy differences give an equilibrium distribution at 25 °C of 31.7%  $C_{2v}$ , 37.6%  $C_2$ , and 30.7%  $C_s$ , in better agreement with experiment than the predictions of all the other calculations. Moreover, these energy differences would be further reduced if geometry optimisation were carried out with this basis set. It appears, therefore, that basis improvements, particularly in expanded polarisation space, will lower the energies of the  $C_2$  and  $C_s$  conformers more than the energy of the  $C_{2v}$  conformer, bringing the theoretical results into agreement with the experimental data.

We now compare the experimental geometries and ionisation energies with the calculated values. In this discussion we use the data obtained from our original DZP

basis, since the results with the other basis sets are not significantly different. Although the DZP basis is not able to provide an accurate estimate of the conformer energy differences, it is expected to give a good estimate of the molecular geometries and ionisation energies of the individual conformers [26,28,30,32].

Table 6 shows the bond lengths, bond angles, and dihedral angles predicted for the three conformers. The calculations would be expected to give bond lengths to within 0.02 Å (usually slightly too short) and bond angles to within 1 or 2° of experimentally determined values [28,30]. Where only one of two possible values is given (e.g., for the C–H bond lengths in the  $C_s$  conformer), it is the average value. The calculated geometrical parameters agree well with the GED data. The increase in the PCP angle in the  $C_{2v}$  conformer relative to that in the  $C_2$  and  $C_s$  structures is noteworthy. It can probably be attributed to an attempt to relieve the repulsion between the phosphane hydrogen atoms, although the relief of lone pair repulsion is probably also a factor.

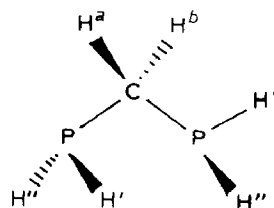
The calculated IEs are shown in Table 7. Usually the Koopmans' IEs calculated with this sort of basis set are slightly too large in absolute value (ca. 10%), although their relative values are normally sufficiently accurate to assist in assignment of PE spectra [30,32].

Simple qualitative valence theory predicts ten valence ionisation energies. Thus, methylenebis(phosphane) would be expected to have two phosphorus lone pair orbitals, four P–H, two C–H, and two C–P bonding orbitals.

Contrary to the usual expectations, the Koopmans' ionisation energies of methylenebis(phosphane) seem to be slightly smaller than the experimental IEs (compare Tables 1 and 7). The two lowest IEs of all three conformers are for the phosphorus lone pair orbitals. Assignment of the remaining orbitals is less straightforward, owing to the delocalisation of the canonical molecular orbitals over the entire molecule. Although an assignment in terms of localised orbitals is therefore an oversimplification, for all three conformers it is reasonable to assign the next four ionisation energies to the P–H bonding orbitals. After this come the two C–H bonding orbitals and, finally, the C–P bonding orbitals.

The most striking feature of the calculated IEs is the difference between the lone pair splitting in the  $C_{2v}$  conformer and that in the  $C_2$  and  $C_s$  conformers. The PE spectrum indicates a small splitting, in line with the theoretical data for the  $C_2$  and  $C_s$  conformers. Here, then, the theoretical data suggest either a  $C_2$  or  $C_s$  geometry.

*Note Added in Proof.* After this paper had been submitted, we learned of the Supplementary Material for ref. 20. This shows that Schleyer and coworkers considered three conformers of  $\text{CH}_2(\text{PH}_2)_2$ , namely I, II, and also the *syn, gauche*



(IV)

$C_1$  conformer (IV). The SCF 3-21G\* optimised geometry of IV had  $\tau$  ca. 72 and 180°. The conformer IV was predicted to be 1.5 kJ mol<sup>-1</sup> lower in energy than I, which in turn was 2.1 kJ mol<sup>-1</sup> more stable than II.

We therefore carried out an SCF calculation on IV with our initial DZP basis set at the 3-21G\* geometry obtained in ref. 20; this showed IV to be 1.0 kJ mol<sup>-1</sup> lower in energy than I with the same basis set. We have not made further calculations on IV, because the energy differences of I-IV are so small that manageable calculations are not expected to be definitive.

Our calculation on the  $C_1$  conformer IV gave Koopmans' *IE*s of 9.75, 10.02, 13.15, 13.76, 14.05, 15.90, 16.63, 21.26, 22.88, and 27.45 eV; which are close to those for the  $C_2$  and  $C_s$  conformers (Table 7). Hence, the experimental *PE* data do not exclude significant contribution from the  $C_1$  conformer.

In the GED analysis, similar arguments which were used to exclude significant contributions from the  $C_{2v}$  conformer apply to the *syn-gauche*  $C_1$  conformation: the calculated distribution of non-bonded P...H distances does not agree with experiment. Hence contributions larger than 20% of  $C_1$ ,  $C_{2v}$ , or both conformers are ruled out.

## References

- 1 Cf. O. Stelzer in E.J. Griffith and M. Grayson (Eds.), Topics in Phosphorus Chemistry, J. Wiley, New York, 1977, Vol. 9, p. 1; C.A. McAuliffe and W. Levason, Phosphine, Arsine and Stibine Complexes of the Transition Elements, Elsevier, Amsterdam, 1979.
- 2 J.A. Connor, J.P. Day, E.M. Jones, and G.K. McEwen, J. Chem. Soc., Dalton Trans., (1973) 347; M.M. Olmstead, C.L. Lee, and A.L. Balch, Inorg. Chem., 21 (1982) 2712; M. Cowie and S.K. Dwight, *ibid.*, 18 (1979) 1209; A.M. Bond, R. Colton, and J.J. Jackowski, *ibid.*, 14 (1975) 274; D.J. Brauer, P.C. Knüppel, and O. Stelzer, Chem. Ber., 120 (1987) 81.
- 3 Cf. J.T. Magee, Inorg. Chem., 8 (1969) 1975; A.L. Balch, J.W. Labadie, and G. Delker, *ibid.*, 18 (1979) 1224.
- 4 D.J. Brauer, S. Hietkamp, H. Sommer, and O. Stelzer, Angew. Chem., Int. Ed. Engl., 96 (1984) 734; D.J. Brauer, S. Hietkamp, H. Sommer, O. Stelzer, G. Müller, and C. Krüger, J. Organomet. Chem., 288 (1985) 35; D.J. Brauer, S. Hietkamp, H. Sommer, O. Stelzer, G. Müller, M. J. Romao, and C. Krüger, *ibid.*, 296 (1985) 411; D.J. Brauer, P.C. Knüppel, and O. Stelzer, J. Chem. Soc., Chem. Commun., (1986) 551.
- 5 Cf. R.J. Puddephatt, Chem. Soc. Rev., 12 (1983) 99.
- 6 (a) V.P. Novikov, V.I. Kolomeets, A.V. Golubinski, L.V. Vilkov, O.A. Raevskii, Z.S. Novikova, and A.N. Kurkin, Zhur. Strukt. Khim., 27 (1986) 39; (b) V.P. Novikov, V.I. Kolomeets, L.V. Vilkov, A.V. Yarkov, O.A. Raevskii, A.N. Kurkin, and Z.S. Novikova, *ibid.*, 27 (1986) 44; (c) V.P. Novikov, A.V. Yarkov, I.O. Umarova, O.A. Raevskii, A.N. Kurkin, and Z.S. Novikova, Izv. Akad. Nauk SSSR, Ser. Khim., (1983) 2252.
- 7 D.W.H. Rankin, H.E. Robertson, and H.H. Karsch, J. Mol. Struct., 77 (1981) 121.
- 8 S. Hietkamp, H. Sommer, and O. Stelzer, Chem. Ber., 117 (1984) 3400.
- 9 H.H. Karsch and H. Schmidbaur, Z. Naturforsch. B, 32 (1977) 762.
- 10 Z.S. Novikova, A.A. Prishchenko, and I.F. Lutsenko, Zh. Obshch. Khim., 47 (1977) 775.
- 11 H. Oberhammer, Molecular Structure by Diffraction Methods, The Chemical Society, Burlington House, London 1976, Vol. 4, p. 24.
- 12 H. Oberhammer, H. Willner, and W. Gombler, J. Mol. Struct. 70 (1981) 273.
- 13 J. Haase, Z. Naturforsch. A, 25 (1970) 936.
- 14 A.G. Maki, R.L. Sams, and W.B. Olson, J. Chem. Phys., 58 (1973) 4502.
- 15 L.S. Bartell, J. Chem. Phys., 32 (1960) 832.
- 16 D.W.H. Rankin, M.R. Todd, and M. Fild, J. Chem. Soc., Dalton Trans., (1982) 2079.
- 17 J. Weidlein, Ü. Müller, K. Dehnicke, Schwingungsspektroskopie, Georg Thieme Verlag, Stuttgart, 1982.

- 18 D. Christen, *J. Mol. Struct.*, 48 (1978) 101.
- 19 J.A. Lannon and E.R. Nixon, *Spectrochim. Acta A*, 23 (1967) 2713.
- 20 P. v. R. Schleyer, E.D. Jemmis, and G.W. Spitznagel, *J. Am. Chem. Soc.*, 107 (1985) 6393.
- 21 M.F. Lappert, J.B. Pedley, B.T. Wilkins, O. Stelzer, and E. Unger, *J. Chem. Soc., Dalton Trans.*, (1975) 1207.
- 22 J.P. Maier and D.W. Turner, *J. Chem. Soc., Faraday Trans. II*, (1972) 711.
- 23 A.H. Cowley, M.J.S. Dewar, D.W. Goodman, and M.C. Padolina, *J. Am. Chem. Soc.*, 96 (1974) 2682.
- 24 A.H. Cowley, M.J.S. Dewar, D.W. Goodman, and M.C. Padolina, *J. Am. Chem. Soc.*, 96 (1974) 3666.
- 25 T.H. Dunning, *J. Chem. Phys.*, 53 (1970) 2823.
- 26 T.H. Dunning and P.J. Hay, in H.F. Schaefer (Ed.), *Methods of Electronic Structure Theory*, Plenum, New York 1977.
- 27 A.D. McLean and G.S. Chandler, *J. Chem. Phys.*, 72 (1980) 5639.
- 28 W.J. Hehre, L. Radom, P. v. R. Schleyer, and J.A. Pople, *Ab Initio Molecular Orbital Theory*, J. Wiley, New York, 1986.
- 29 P. Pulay, in H.F. Schaefer (Ed.), *Applications of Electronic Structure Theory*, Plenum, New York 1977.
- 30 P. Carsky and M. Urban, *Ab Initio Calculations: Methods and Applications in Chemistry*, Springer-Verlag, Berlin, 1980.
- 31 J.A. Pople, R. Krishnan, H.B. Schlegel, and J.S. Binkley, *Int. J. Quantum Chem. Symp.*, 13 (1979) 225.
- 32 M.E. Schwartz, in H.F. Schaefer (Ed.), *Applications of Electronic Structure Theory*, Plenum, New York, 1977.